A new damage index for plane steel frames exhibiting strength and stiffness degradation under seismic motion

George S. Kamaris[a], George D. Hatzigeorgiou[b,*], Dimitri E. Beskos[a,c]

[a] Department of Civil Engineering, University of Patras, GR-26500 Patras, Greece.

[b] Department of Environmental Engineering, Democritus University of Thrace, GR-67100 Xanthi, Greece.

[c] Office of Theoretical and Applied Mechanics, Academy of Athens, 4 Soranou Efessiou, GR-11527 Athens, Greece.

Abstract

A new damage index for plane steel frames under earthquake ground motion is proposed. This index is defined at a section of a steel member and takes into account the interaction between the axial force N and bending moment M acting there. This interaction is defined by two curves in the N-M plane. The first curve is the limit between elastic and inelastic material behavior, where damage is zero, while the second one is the limit between inelastic behavior and complete failure, where damage is equal to one. The damage index is defined by assuming a linear variation of damage between the two abovementioned curves. Thus, for a given N-M combination at a member section, obtained with the aid of a two dimensional finite element program, one easily defines the damage index of that section. Material nonlinearities are taken into account by a stress-strain bilinear model including cyclic strength and stiffness degradation in the framework of lumped plasticity (plastic hinge model), while geometrical nonlinearities are modeled by including large deflection effects. The increase of damage related to strength reduction due to low-cycle fatigue is also taken into account. Several illustrative examples serve to demonstrate the use of the proposed damage index and to compare it with other well known damage indices.

[*] : Corresponding author: Tel.: +30.25410.79373; Fax: +30.25410.79373
E-mail address: gchatzig@duth.gr

1. Introduction

Damage in a structure under loading can be defined as the degradation or deterioration of its integrity resulting in reduction of its load capacity. In earthquake-resistant design of structures, some degree of damage in the structural members is generally accepted. This is done because the cost of a structure designed to remain elastic during a severe earthquake would be very large. Thus, existing seismic codes, e.g., EC8 [1], in an implicit way and more recent performance-based seismic design methods [2,3] in an explicit and more systematic way employ the concept of damage to establish structural performance levels corresponding to increasing levels of earthquake actions. These performance levels mainly describe the damage of a structure through damage indices, such as the interstory drift ratio (IDR), or the member plastic rotations.

Several methods to determine damage indices as functions of certain response parameters have been presented in the literature. In general, these methods can be noncumulative or cumulative in nature. The most commonly used parameter of the first class is ductility, which relates damage only to the maximum deformation and is still regarded as a critical design parameter by codes. To account for the effects of cyclic loading, simple rules of stiffness and strength degradation have been included in further noncumulative indices [4,5,6], mainly referred to reinforced concrete members. Cumulative-type indices can be divided in deformation based [7] or hysteretic based [8, 9] formulations and methods that consider the effective distribution of inelastic cycles and generalize the linear law of low-cycle fatigue of metals, in a hypothesis of linear damage accumulation [10]. Combinations of deformation and energy dissipation have been also proposed to establish damage indices [11]. In these methods damage is expressed as a linear combination of the damage caused by excessive deformation

2

and that contributed by repeated cyclic loading effects [11]. Finally, the concept of continuum damage mechanics [12] in conjunction with the finite element method of concentrated inelasticity has been employed in the analysis of steel and reinforced concrete structures [13,14] for the determination of their damage. In this paper, a new damage index for plane steel frames under earthquake ground motion is proposed.

2. Hysteresis models that incorporate strength and stiffness degradation

Several hysteresis models have been proposed in the literature. Some of them have hysteresis rules that account for stiffness degradation by modifying the path by which the reloading branch approaches the backbone curve, e.g., the peak oriented model [15] or various 'pinching' models [16]. In 1970, Takeda [16] developed a model with a trilinear backbone curve that degrades the unloading stiffness based on the maximum displacement of the system. In addition, smooth hysteresis models have been developed that include a continuous change of stiffness due to yielding, and sharp changes due to unloading, e.g. the Wen–Bouc model [17]. The need to model both stiffness and strength degradation led to the development of more versatile models like those of Sivaselvan and Reinhorn [18], which include rules for stiffness and strength degradation as well as pinching. Song and Pincheira [19] developed a model that is capable of representing cyclic strength and stiffness degradation based on dissipated hysteretic energy. This is essentially a peak-oriented model that considers pinching based on degradation parameters. Erberik and Sucuoğlu [20] and Sucuoğlu and Erberik [21] developed low-cycle fatigue, hysteresis and damage models for deteriorating systems on the basis of test data and analysis. Ibarra et al. [22] created a model in which four modes of cyclic degradation are defined with respect to the backbone curve based on the hysteretic response of the component. This was improved later by Lignos and Krawinkler [23]. In the commercial computer program Ruaumoko [24] stiffness and strength degradation can be taken into account through a linear function that depends on the inelastic cycles a

member sustains. This model is described next and used in this work because of its simplicity and agreement with experiments.

Ruaumoko [24] is a program that performs nonlinear dynamic analysis with the aid of the finite element method. It utilizes, among others, a material behavior model that takes into account strength degradation with the number of inelastic cycles, n. More specifically, for the two dimensional (2D) case, the reduced strength in each loading direction is obtained by multiplying the initial strength by a parameter, which is a linear function of the number of inelastic cycles. This parameter f is given by the equation

$$f = \frac{S_r - 1}{n_2 - n_1}(n - n_1) + 1 \tag{1}$$

where n_1 is the cycle at which degradation begins, n_2 the cycle at which degradation stops and S_r the residual strength factor that multiplies the initial yield strength to produce the residual strength. It is assumed that the stiffness deteriorates so that the yield displacement remains constant.

For the calibration of the above material model of Ruaumoko 2D [24], results from experiments performed by Ricles et al. [25] at the ATLSS laboratory of Lehigh University were used. These experiments focused on the cyclic inelastic performance of full-scale welded unreinforced flange moment connection specimens.

The beam size for all specimens was a W36x150 section of A572 Grade50 steel. Six exterior connection specimens (Specimens T1, T2, T3, T4, T5 and T6) and five interior connection specimens (Specimens C1, C2, C3, C4 and C5) were tested. For the exterior connection, one W36x150 beam was connected to the flange of a W14x311 A572 Grade 50 column. A pair of parallel horizontal actuators were placed at the top of the column to impose the story drift to the specimen. The displacement history followed the SAC Protocol [26]. A test was terminated when either fracture occurred, resulting

in a significant loss of capacity, or after reaching an interstorey drift ratio of 0.06 radians. In order to prevent the out-of-plane movement and twisting of the beam and column, lateral bracing was provided. The setup of the experiment is shown in Fig. 1.

The experiment for specimen C2 was simulated by Ruaumoko 2D [24] and the moment-rotation curves of the right beam of the connection were evaluated. The experimental curve is shown in Fig. 2, together with the one simulated by Ruaumoko 2D [24]. The agreement between the experimental and the numerical curves is considered to be satisfactory.

It should be noticed herein that the displacement protocol used in the adopted experiment is cyclic with monotonically increasing cyclic displacement amplitudes. This is the case with the majority of the experiments conducted and published in the pertinent literature, such protocols are utilised. For example, SAC [26] proposes two different loading history protocols, the standard SAC and the near-fault one with each one of them leading to a different structural response. However, the energy dissipation capacity, which is related to structural damage, is insensitive to the different types of loading protocols in the case of steel structures [27].

3. Proposed damage index

In this section the proposed damage index is presented. It is defined at a section of a steel member and has the following form:

$$D_S = \frac{c}{d} = \frac{\sqrt{(M_S - M_A)^2 + (N_S - N_A)^2}}{\sqrt{(M_B - M_A)^2 + (N_B - N_A)^2}} \tag{2}$$

In the above, the bending moments M_A, M_S and M_B and the axial forces N_A, N_S and N_B as well as the distances c and d are those shown in the bending moment M - axial force N interaction diagram of

Fig. 3 for a plane beam-column element. The proposed damage index takes into account the interaction between the bending moment M_S and axial force N_S acting at the specific section S at a certain time during the loading history.

Figure 3 includes a lower bound damage curve, the limit between elastic and inelastic material behavior and an upper bound damage curve, the limit between inelastic behavior and complete failure. Thus, damage at the former curve is zero, while at the latter curve is one. Equation (2) is based on the assumption that damage evolution varies linearly between the above two damage bounds. Points (M_A, N_A) and (M_B, N_B), can be found by drawing a line that connects point (M_S, N_S) to the origin of the axes. The intersection of the lower and upper bound damage curves to the above line determines the abovementioned points.

The lower bound curve of Fig. 3 is the one found in finite element programs of lumped plasticity and indicates the formation of a plastic hinge at a member. In the Ruaumoko program [24], used herein, this lower bound curve is described as

$$\frac{0.88M}{f \cdot M_{pl}} + \frac{N}{f \cdot N_{pl}} = 1 \quad for \quad M \le 0.9M_{pl} \quad and \quad N \le 0.2N_{pl}$$

$$\frac{M - M_{pl}}{f \cdot M_{pl}} + \frac{N}{f \cdot N_{pl}} = 1 \quad for \quad M > 0.9M_{pl} \quad and \quad N > 0.2N_{pl}$$

(3)

where N_{pl} and M_{pl} are given by the expressions

$$M_{pl} = f_y W_{pl}, \quad N_{pl} = f_y A$$

(4)

with f_y being the yield stress of steel, W_{pl} the section plastic modulus and A the sectional area.

6

The upper bound curve of Fig. 3 has a similar form with the *M-N* interaction formula given in EC3 [28] provisions, with the hardening effect not taken into account, i.e., with $\sigma_u = \sigma_y$ or equivalently, $N_u = N_y$. Thus, this curve can be expressed as

$$\frac{M}{f \cdot M_u} + \left(\frac{N}{f \cdot N_u} \right)^2 = 1 \tag{5}$$

where N_u and M_u are the ultimate axial force and bending moment, respectively, which cause failure of the section and are equal to

$$M_u = f_u W_{pl}, \quad N_u = f_u A \tag{6}$$

with f_u being the ultimate stress of steel. The factor f in Eqs (3) and (6) is the scale factor of Eq. (1) that is used so as phenomena of strength and stiffness degradation to be taken into account.

The increase of damage related to strength reduction due to low-cycle fatigue is taken into account by following the work of Sucuoğlu and Erberik [21]. Thus, an amount of damage ΔD_s, related to this phenomenon, is added to damage, D_s, computed by Eq. (2). Here the case that the axial force is zero is examined and thus the damage can be expressed with the aid of Eq. (2) as

$$D_S = \frac{M_S - M_y}{M_u - M_y} = \left(\frac{k_f}{\frac{M_u}{M_y} k_o - k_f} \right) \left(\frac{M_S}{M_y} \frac{k_o}{k} - 1 \right) \tag{7}$$

where k_o is the initial elastic stiffness, k_f is the secant stiffness at the ultimate rotation θ_u of the current cycle and k is the secant stiffness at the current cycle.

7

Figure 4 shows the moment yield values M_y and M_y^n at the constant amplitude yield rotation θ_y, which correspond to the 1st and nth positive cycle, respectively. Accordingly, k_1 and k_n are the corresponding effective stiffnesses, which are substituted for k in Eq. (7) in order to determine the damages D_{s1} και D_{sn}, in the 1st and nth cycle, respectively. Eventually, the moment M_s at the 1st cycle reduces to M_s^n at the nth cycle by an amount ΔM_n, leading to an increase in damage due to the associated reduction in the effective stiffness from k_1 to k_n according to Eq. (7). The projection of the point A´, which is the intersection of lines B´A´ and AA´, on the rotation axis, θ'_m, indicates that the same amount of damage would be experienced at the nth cycle if the system were pushed to the rotation θ'_m to reach the moment M_s'. Hence, Eq. (7) yields the associated damage D_{sn} at the nth cycle when M_s is replaced by M_s'. In this case, the moment M_s' is composed of the moment M_s and an additional moment ΔM_s arising from strength loss. Thus, an amount of damage ΔD_s should be added to the system due to the moment increase which is equal to

$$\Delta D_S = \frac{M_s' - M_s}{M_u - M_y} \tag{8}$$

This methodology can be extended to the case that the axial force is not zero. In this case the additional moment due to strength loss is found in the same way as above and the total damage is calculated as the sum of the damage of Eq. (2) and the ΔD_s.

The calculation of ΔD_s, following the aforementioned methodology, is difficult and impractical for plane steel frameworks seismically analyzed by the Ruaumoko [24] program. For this reason, ΔD_s was calculated with the aid of results of extensive parametric studies on a cantilever beam under cyclic excitation conducted with the aid of the Ruaumoko program [24]. The cantilever beam consisted of various standard HEB and IPE sections (40 of them) and the excitation history followed the SAC Protocol [26]. Thus, an empirical equation that gives ΔD_s as a function of the number of inelastic

8

cycles n and the damage D_s the member has sustained in the current cycle was constructed. More specifically, in every loading cycle, the damage index D_s and the damage increment ΔD_s were calculated according to Eqs (2) and (8), respectively. Then, a databank of the results was formed and analyzed with the aid of nonlinear regression analysis, leading to the following expression for ΔD_s:

$$\Delta D_s = 0.56 \cdot n^{0.292} \cdot D_s^{0.914} \tag{9}$$

Consequently, for a combination of moment M_S and axial force N_S computed at a member section, one can easily evaluate the damage index there by using Eqs (2) and (9) at each time step of a nonlinear dynamic analysis. It is supposed that the damage index at a section is the maximum value of all its values calculated at each time step. The calculation of M-N pairs is conducted with the aid of the Ruaumoko 2D finite element program [24]. In this program, material nonlinearities are taken into account through a bilinear moment-rotation model that incorporates strength and stiffness degradation in the framework of lumped plasticity (plastic hinge model), while, geometrical nonlinearities are modeled by including large displacement effects. Finally, the computation of the proposed damage index, is accomplished with the aid of a computer program in FORTRAN created by the authors.

4. Other damage indices

The proposed damage index will be compared with five other damage indices existing in the literature. These are the damage indices of Park and Ang [11], Bracci et al. [9], Roufaiel and Meyer [5], Cosenza and Manfredi [6] and Banon and Veneziano [4]. These indices have been selected here because i) are the most widely used in applications and ii) can be easily employed with the aid of the Ruaumoko 2D program [24]. In the following, a brief description of all these five damage indices will be given for reasons of completeness.

The damage index D_{PA} of Park and Ang [11] is expressed as a linear combination of the damage caused by excessive deformation and that contributed by repeated cyclic loading effects, as shown in the following equation:

$$D_{PA} = \frac{\delta_m}{\delta_u} + \frac{\beta}{Q_y \delta_u} \int dE \qquad (10)$$

In the above, the first part of the index is expressed as the ratio of the maximum experienced deformation δ_m to the ultimate deformation δ_u under monotonic loading. The second part is defined as the ratio of the dissipated energy to the term $\beta/(Q_y \delta_u)$, where Q_y is the yield strength and the coefficient β is a non-negative parameter determined from experimental calibration. In this paper β is taken equal to 0.025, which is a typical value for steel structures [29].

Bracci et al. [9] suggested a damage index equal to the ratio of 'damage consumption' (loss in damage capacity) to 'damage potential' (capacity), defined as appropriate areas under the monotonic and the low-cycle fatigue envelopes. Thus, the 'damage potential'. D_P, is defined as the total area between monotonic load–deformation curve and the fatigue failure envelope. As damage proceeds, the load–deformation curve degrades, resulting in the damage D_s due to the loss of strength and the irrecoverable deformation causes deformation damage D_D. Thus, this damage index D_B is expressed as

$$D_B = \frac{D_D + D_S}{D_P} \qquad (11)$$

Roufaiel and Meyer [5] proposed that the ratio between the secant stiffness at the onset of failure M_m/φ_m and the minimum secant stiffness reached so far M_x/φ_x, can be used as a good indicator of

damage. Based on that, they defined their damage index D_{RM} as the modified flexural damage ratio (*MFDR*) of the form

$$D_{RM} = MFDR = \max[MFDR^+, MFDR^-] \tag{12}$$

$$MFDR^+ = \frac{\phi_x^+}{M_x^+} - \frac{\phi_y^+}{M_y^+} \Bigg/ \frac{\phi_m^+}{M_m^+} - \frac{\phi_y^+}{M_y^+}, \quad MFDR^- = \frac{\phi_x^-}{M_x^-} - \frac{\phi_y^-}{M_y^-} \Bigg/ \frac{\phi_m^-}{M_m^-} - \frac{\phi_y^-}{M_y^-} \tag{13}$$

where ϕ is the beam curvature due to a bending moment M, the term M_y/ϕ_y is the initial elastic stiffness and subscripts + and – denote the loading direction.

The Consenza and Manfredi [6] damage index is defined as

$$D_{CM} = \frac{\mu - 1}{\mu_{u,mon} - 1} \tag{14}$$

where μ is the maximum ductility during the loading history and $\mu_{u,mon}$ is the maximum allowable value of ductility equal to $x_{u,mon}/x_y$. with the $x_{u,mon}$ being the ultimate displacement given by monotonic tests and x_y the yield displacement. For members that are under flexure, μ, $\mu_{u,mon}$, $x_{u,mon}$ and x_y are replaced by μ_θ, $\mu_{\theta,mon}$, $\theta_{u,mon}$, and θ_y, respectively. The terms μ_θ, $\mu_{\theta,mon}$ are the rotation ductility during the loading history and the maximum allowable value of rotation ductility under monotonic tests, respectively, while $\theta_{u,mon}$, and θ_y are the ultimate and the yield rotation, respectively.

The Banon and Veneziano [4] analysis is set in a probabilistic context and the model has been calibrated on the basis of 29 different tests on reinforced concrete elements and structures, selected from among the most representative ones in the technical literature. In particular, the damage parameters d_1 and d_2 are defined, respectively, as the ratio of stiffness at yielding point to secant stiffness at failure, and the plastic dissipated energy E_h normalized with respect to the absorbed energy

at the elastic limit. If the elastic-plastic model is used, d_1 is obviously equal to the ratio of the maximum displacement to the displacement x_{max} at the elastic limit x_y. Therefore, according to the notation introduced above, parameters d_1 and d_2 can be expressed as

$$d_1 = x_{max}/x_y, \quad d_2 = E_h/(1/2)F_y x_y \tag{15}$$

where F_y is the yield strength. Furthermore, modified damage parameters d_1^* and d_2^* are introduced of the form

$$d_1^* = d_1 - 1, \quad d_2^* = ad_2^b \tag{16}$$

where a and b are two parameters which characterize the structural problem and are defined experimentally. For flexure, x and F are replaced by θ and M, respectively. Thus, the damage index D_{BV} is defined as

$$D_{BV} = \sqrt{(d_1^*)^2 + (d_2^*)^2} \tag{17}$$

5. Examples and comparisons

In this section, two numerical examples are presented in order to demonstrate the use of the proposed damage index and compare it with the five well known damage indices briefly described in the previous section.

5.1. Three storey steel frame

A plane three storey - three bay steel frame, as shown in Fig. 5, is examined in this example. The bay width is assumed equal to 5 m and the story height equal to 3 m. Columns consist of standard HEB240 sections and beams of standard IPE330 sections. The frame is subjected to the uniform load 27.5kN/m (dead and live loads of floors), while the material properties correspond to structural steel grade S235. The frame has been designed in accordance with the provisions of EC3 [28] and EC8 [1] and its fundamental natural period is equal to 0.73 sec. The expected ground motion is defined by the elastic acceleration design spectrum of the EC8 seismic code [1], with a peak ground acceleration equal to 0.4 g and a soil class B. The SAP2000 [30] software package has been used for elastic analysis and steel design.

For this frame, incremental nonlinear dynamic analyses (IDA) were performed with the aid of the Ruaumoko 2D program [24]. The frame was excited with seven (7) ground motions, which were scaled in order that several performance levels to be reached until the state of dynamic instability and collapse. Table 1 shows the ordinary seismic motions used in this example and Fig. 6 depicts the curves of maximum interstorey drift ratios (IDR) versus the peak ground acceleration (PGA) values of the seven (7) ground motions. Collapse is indicated through the plateau that is formed in those curves after a certain value of PGA.

Figures 7 and 8 show the five damage indices of Section 4 together with the proposed one as functions of the peak ground acceleration, for ground motions 1 and 4 of Table 1, respectively. The first figure refers to damage of beam B of the first floor of the frame (see Fig. 5) and the second one to damage of column C of the first floor of the same frame. It is observed that the proposed damage index is in between the others and close to those of Bracci et al. [9] and Cosenza and Manfredi [6] for small values of peak ground acceleration. This comes from the fact that these damage indices are associated with the ratio of demand to capacity, i.e. they are defined in a similar manner with the proposed one. For larger values of the peak ground acceleration, for which the frame has sustained extensive plastification, the proposed damage index is very close to Park and Ang [11], Roufaiel and Meyer [5]

13

and Banon and Veneziano [4] damage indices, which account for the combination of maximum displacement and energy dissipation as an indicator of damage. This is because the extensive plastification corresponds to a larger number of inelastic cycles, which lead to an increase of the proposed damage index as indicated by Eq. (9). This increase is reasonable, because the more a member gets in the plastic region and its capacity reduces, the more its damage increases, something that is satisfied by the proposed damage index. In addition, for very large values of peak ground acceleration the proposed damage index is larger than the Bracci et al. [9] and Cosenza and Manfredi [6] damage indices, which do not take into account the effects of low-cycle fatigue. The same results are observed at the other members of the frame and for the other motions of Table 1, but they are not presented herein due to lack of space.

Finally, Figs 9-13 show the correlation between the five damage indices of Section 4 and the proposed one that corresponds to all columns of the frame under consideration for all the ground motions. The correlation of the proposed damage index to the other damage indices is considered to be satisfactory as it provides values for the correlation coefficient R^2 between 0.74-0.88, with the larger correlation to be with the Cosenza and Manfredi [6] damage index, where R^2 was equal to 0.88. However, the R factor is not the single parameter that can examine the correlation between the existing damage indices with the proposed one. Perhaps, the simplest relation, between an existing (x) and the proposed damage index (y) is

$$y=ax \tag{18}$$

where the slope a can be evaluated applying linear regression analysis using the least squares method. It is obvious that a slope close to unity means a higher level of correlation, as in the case of Park and Ang [11], Roufaiel and Meyer [5] and Banon and Veneziano [4] damage indices. However, some discrepancies appear in the results concerning Bracci et al. [9] and Cosenza and Manfredi [6] damage

14

indices, although the correlation coefficient R^2 provided in these cases is satisfactory. The slope a of equation Eq. 18 shown in Fig. 10 and 12 differs from unity by 24% (a=1.24) and 45% (a=1.45) for Bracci et al. [9] and Cosenza and Manfredi [6] damage indices, respectively. This means that the values of the proposed damage index are in general larger than those of the other two existing damage indices and these differences have mainly to do with the inability of these existing damage models to consider strength deterioration, which generally leads to higher damage values in comparison with those for non-deteriorating models.

For all beams of the frame, from analogous figures not shown here due to space limitations, the correlation was found to be slightly better with R^2 to vary between the values of 0.79-0.88, with the best correlation to be with the Cosenza and Manfredi [6] damage index where R^2 was equal to 0.88.

In addition, the correlation between the proposed damage index and the other five ones for the columns and beams of the first floor was computed. The first floor was selected because the axial forces of the columns there are larger than those of the other floors and thus their influence was expected to be larger. In this case, the correlation coefficient R^2 between the proposed damage index and that of Park and Ang [11] equals 0.70 and 0.78 for the columns and beams, respectively, indicating a better correlation for the beams than the columns. The same trend was observed for the correlation between the proposed damage index and the other damage indices. This better correlation for the beams can be attributed to the fact that in beams axial forces and hence moment-axial force interaction effects, taken into account by the proposed damage index but not by the other ones, are less important than in columns.

5.2. *Six storey steel frame*

A plane six storey - three bay steel frame is examined here. The bay width is assumed equal to 5 m and the story height equal to 3 m as shown in Fig. 14. Columns consist of standard HEB300 sections and beams of standard IPE360 sections for the first three floors, while standard HEB360 and IPE330

sections for the columns and beams, respectively, were used for the rest of the floors. The values of the uniform load on the beams of the frame and the yield stress of the steel are the same with those of the previous example. The frame has been designed in accordance with the provisions of EC3 [28] and EC8 [1] and its fundamental natural period is equal to 1.17 sec. The SAP2000 [30] software package has been used for elastic analysis and steel design.

For this frame, incremental nonlinear dynamic analyses (IDA) were performed with the aid of the Ruaumoko 2D program [24]. The frame was excited with the seven (7) ground motions of Table 1, which were scaled again so as several performance levels to be reached until collapse. Figure 15 depicts the curves of IDR versus PGA for the ground motions considered.

Figures 16 and 17 show the five damage indices of Section 4 together with the proposed one as functions of the peak ground acceleration, for ground motions 1 and 3 of Table 1, respectively. The first figure refers to damage of beam B of the first floor of the frame (see Fig. 14) and the second one to damage of column C of the first floor of the same frame. One can observe again that the proposed damage index is in between the others, close to those of Bracci et al. [9] and Cosenza and Manfredi [6] for small values of PGA and very close to Park and Ang [11], Roufaiel and Meyer [5] and Banon and Veneziano [4] damage indices for larger values of PGA. This behavior can be interpreted by the same reasoning as in the previous example. It was also found that, as in the previous example, the correlation coefficient R^2 between the proposed damage index and the other five ones of Section 4 was better for beams than for columns indicating the importance of the moment-axial force interaction effects taken into account by the proposed damage index.

It should be also noted that the proposed damage index for column C, shown in Fig.17, gives larger values of damage than the other five damage indices for a value of PGA greater than 0.6 g corresponding to a value of IDR equal to 0.017. Thus, the proposed model gives higher damage values for maximum inelastic drifts higher than 0.017, compared to the other damage indices. This can be explained by the fact that the proposed damage index takes into account strength and stiffness

16

degradation resulting to higher values of the maximum inelastic displacement, which is physically related to damage. In contrary, the other five damage indices, which are obtained using non-degrading models resulting to smaller values of the maximum inelastic displacement, provide smaller values of damage. Furthermore, Fig. 18 shows two IDA curves of the frame for ground motion 3 of Table 1. The first one corresponds to the proposed degrading model, while the second one to a non-degrading model produced from the proposed one by assuming the parameter f of Eq. (1) to be equal to 1. It is observed that for a value of PGA greater than 0.6 g the values of *IDR* for the degrading system are larger than those for the non-degrading one.

6. Conclusions

On the basis of the preceding developments, the following conclusions can be stated:

1) A new damage index for plane steel moment resisting frames under seismic loading has been developed and efficiently used in conjunction with the finite element method that takes into account material and geometric nonlinearities.

2) The proposed damage index is conceptually simple and realistic because

    - It accounts for the interaction between the axial force and the bending moment at a member section.

    - It incorporates cyclic strength and stiffness deterioration based on a law calibrated with experimental results.

    - It accounts for the phenomenon of low-cycle fatigue, which influences the damage of frames that are subjected to ground motions.

3) In comparison with five well known damage indices in the literature, the proposed damage index provides results in between those indices, is close to those of Bracci et al. and Cosenza and

17

Manfredi for small values of PGA and very close to Park and Ang, Roufaiel and Meyer and Banon and Veneziano damage indices for larger values of PGA.

4) The correlation of the proposed damage index with five well known indices in the literature seems to be satisfactory. The importance of the moment-axial force interaction effects in columns, taken into account only by the proposed damage index, was verified.

REFERENCES

[1] EC8. Design of structures for earthquake resistance, Part 1: General rules, seismic actions and rules for buildings, European Standard EN 1998-1, European Committee for Standardization (CEN), Brussels, 1998.

[2] Fajfar P and Krawinkler H. Seismic Design Methodologies for the Next Generation of Codes. Bled, 24-27 June 1997, Balkema, Rotterdam.

[3] FEMA. FEMA-273 Building Seismic Safety Council, NEHRP guidelines for the seismic rehabilitation of buildings. Federal Emergency Management Agency, Washington (DC), 1997.

[4] Banon H, Veneziano D. Seismic safety of reinforced concrete members and structures. Earthquake Engineering and Structural Dynamics1982; 10:179-173.

[5] Roufaiel MS Meyer C. Analytical modeling of hysteretic behavior of R/C frames. Journal of Structural Engineering, ASCE 1987; 113:429-444.

[6] Cosenza E, Manfredi G, Ramasco R. The use of damage functionals in earthquake engineering: A comparison between different methods. Earthquake Engineering and Structural Dynamics 1993; 22(10):855-868.

[7] Stephens JE, Yao JTP. Damage assessment using response measurements. Journal of Structural Engineering, ASCE 1987; 113:787-801.

[8] McCabe SL, Hall WJ. Assessment of seismic structural damage. Journal of Structural Engineering, ASCE 1989; 115: 2166-2183.

[9] Bracci JM, Reinhorn, AM, Mander JB. Deterministic model for seismic damage evaluation of reinforced concrete structures, Technical Report NCEER 89-0033, State University of New York at Buffalo, 1989.

[10] Krawinkler H, Zohrei M. Cumulative damage in steel structures subjected to earthquake ground motions. Computers and Structures 1983; 16:531-541.

[11] Park Y-J, Ang AH-S. Mechanistic seismic damage model for reinforced concrete. Journal of Structural Engineering, ASCE 1985; 111:722-739.

[12] Lemaitre J. A Course on Damage Mechanics. Springer-Verlag, Berlin, 1992.

[13] Hatzigeorgiou GD, Beskos DE. Direct damage controlled design of concrete structures. Journal of Structural Engineering, ASCE 2007; 133:205-215.

[14] Kamaris GS, Hatzigeorgiou GD, Beskos DE. Direct damage controlled design of plane steel-moment resisting frames using static inelastic analysis. Journal of Mechanics of Materials and Structures 2009; 4:1375-1393.

[15] Clough RW Johnston SB. Effects of stiffness degradation on earthquake ductility requirements. Proceedings of the Japan Earthquake Engineering Symposium, Tokyo, Japan, 1966.

[16] Takeda T, Sozen MA, Nielson NN. Reinforced concrete response to simulated earthquakes. Journal of the Structural Division, ASCE 1970; 96:2557-2573.

[17] Wen, YK. Method for random vibration of hysteretic systems. Journal of the Engineering Mechanics Division, ASCE 1976; 112:249–263.

[18] Sivaselvan MV, Reinhorn AM. Hysteretic models for deteriorating inelastic structures. Journal of Engineering Mechanics, ASCE 2000; 126:633-640.

[19] Song J, Pincheira J. Spectral displacement demands of stiffness and strength degrading systems. Earthquake Spectra 2000; 16:817-851.

[20] Erberik A, Sucuoğlu H. Seismic energy dissipation in deteriorating systems through low-cycle fatigue. Earthquake Engineering and Structural Dynamics 2004; 33: 49-67.

[21] Sucuoğlu H, Erberik A. Energy-based hysteresis and damage models for deteriorating systems. Earthquake Engineering and Structural Dynamics 2004; 33: 69-88.

[22] Ibarra LF, Medina RA, Krawinkler H. Hysteretic models that incorporate strength and stiffness degradation. Earthquake Engineering and Structural Dynamics 2005; 34:1489-1511.

[23] Lignos DG, Krawinkler H. Deterioration Modeling of Steel Components in Support of Collapse Prediction of Steel Moment Frames under Earthquake Loading. Journal of Structural Engineering, ASCE 2011; 137(11): 1291-1302.

[24] Carr AJ. RUAUMOKO-2D. Inelastic Time-History Analysis of Two-Dimensional Framed Structures, Department of Civil Engineering. University of Canterbury, New Zealand, 2006.

[25] Ricles JM, Mao C, Lu L-W, Fisher JW. Development and Evaluation of Improved Details for Ductile Welded Unreinforced Flange Connections. ATLSS Report No: 00-04, Lehigh University, Bethlehem, 2000.

[26] SAC Joint Venture. Protocol for Fabrication, Inspection, Testing, and Documentation of Beam-Column Connection Tests and Other Experimental Specimens. Report No. SAC/BD-97/02, SAC Joint Venture, Sacramento, California, 1997.

[27] Uang CM, Yu QS, Gilton CS. Effects of loading history on cyclic performance of steel RBS moment connections. Proceedings of the 12th WCEE, Upper Hutt, New Zealand; 2000.

[28] EC3. Design of Steel Structures – Part 1-1: General Rules for Buildings, ENV1993-1-1, European Standard EN 1998-1, European Committee for Standardization (CEN), Brussels, 1992.

[29] Castiglioni CA, Pucinotti R. Failure criteria and cumulative damage models for steel components under cyclic loading. Journal of Constructional Steel Research 2009; 65:751-765.

[30] SAP2000. Static and Dynamic Finite Element Analysis of Structures. Version 9.1.4. Computers and Structures Inc., Berkeley, California, 2005.

Table 1 Characteristics of ground motions used in examples.

No.	Date	Record Name	Station Name	PGA (g)
1.	1992/04/25	Cape Mendocino	89509 Eureka	0.154
2.	1992/06/28	Landers	24577 Fort Irwin	0.114
3.	1994/01/17	Northridge	24389 LA - Century City CC North	0.256
4.	1994/01/17	Northridge	24538 Santa Monica City Hall	0.883
5.	1994/01/17	Northridge	24400 LA - Obregon Park	0.355
6.	1994/01/17	Northridge	127 Lake Hughes #9	0.165
7.	1994/01/17	Northridge	24401 San Marino, SW Academy	0.116

Captions of figures

Figure 1. Interior connection steel specimen under cyclic loading.

Figure 2. Moment-rotation hysteresis loops for the specimen of Fig.1.

Figure 3. Bending moment-axial force interaction diagram and definition parameters of proposed damage index.

Figure 4. Increase of damage due to low-cycle fatigue in a moment-rotation diagram.

Figure 5. Geometry of the three storey plane steel frame.

Figure 6. IDA curves of the three storey steel frame under the 7 ground motions of Table 1.

Figure 7. Comparison of various damage indices with the proposed one at beam B of the three storey frame for ground motion 1.

Figure 8. Comparison of various damage indices with the proposed one at column C of the three storey frame for ground motion 4.

Figure 9. Correlation between the proposed damage index and that of Park and Ang that corresponds to all columns of the three storey frame.

Figure 10.   Correlation between the proposed damage index and that of Bracci et al. that corresponds to all columns of the three storey frame.

Figure 11.   Correlation between the proposed damage index and that of Roufaiel and Meyer that corresponds to all columns of the three storey frame.

Figure 12.   Correlation between the proposed damage index and that of Cosenza and Manfredi that corresponds to all columns of the three storey frame.

Figure 13.   Correlation between the proposed damage index and that of Banon and Veneziano that corresponds to all columns of the three storey frame.

Figure 14.   Geometry of the six storey plane steel frame.

Figure 15.   IDA curves of the six storey steel frame under the 7 ground motions of Table 1.

Figure 16.   Comparison of various damage indices with the proposed one at beam B of the six storey frame for ground motion 1.

Figure 17.   Comparison of various damage indices with the proposed one at column C of the six storey frame for ground motion 2.

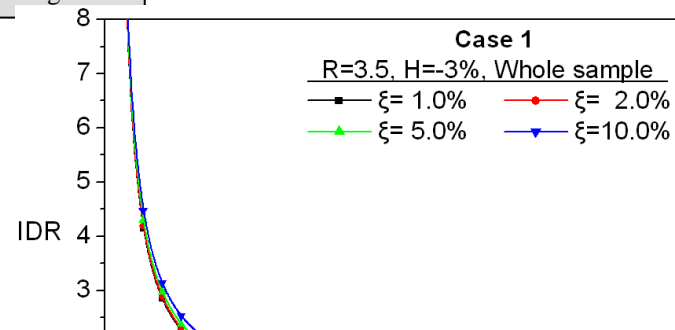Figure 18.   IDA curves for the six storey steel frame under ground motion 3, using a degrading and a non-degrading model
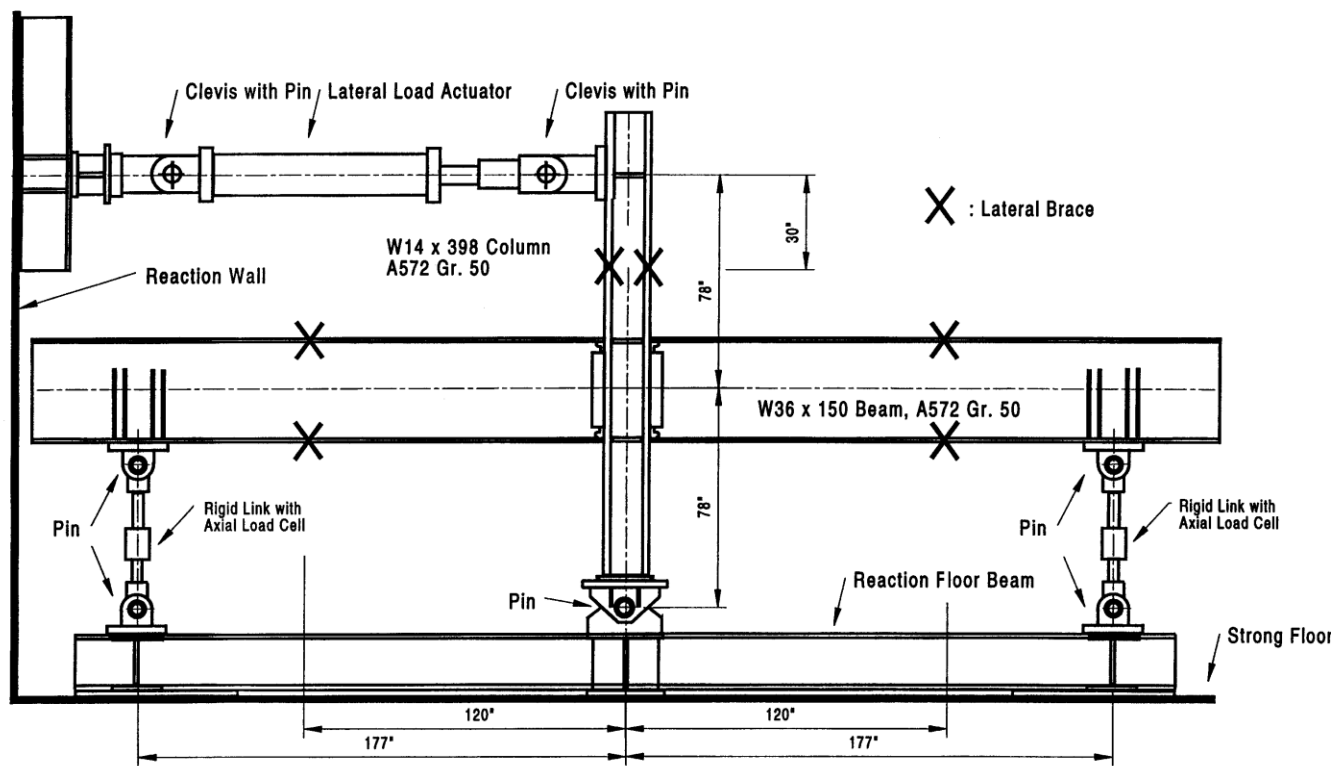
Figure 1
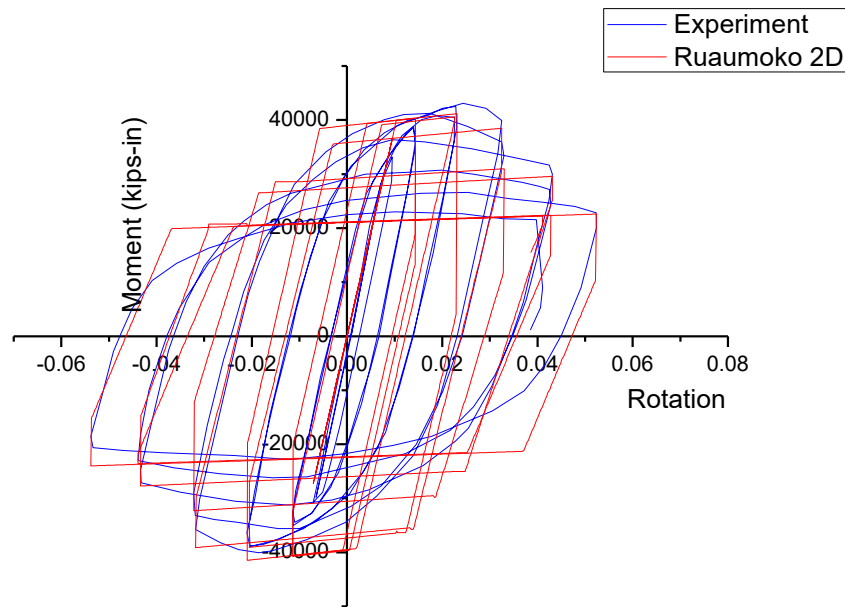
Figure 2
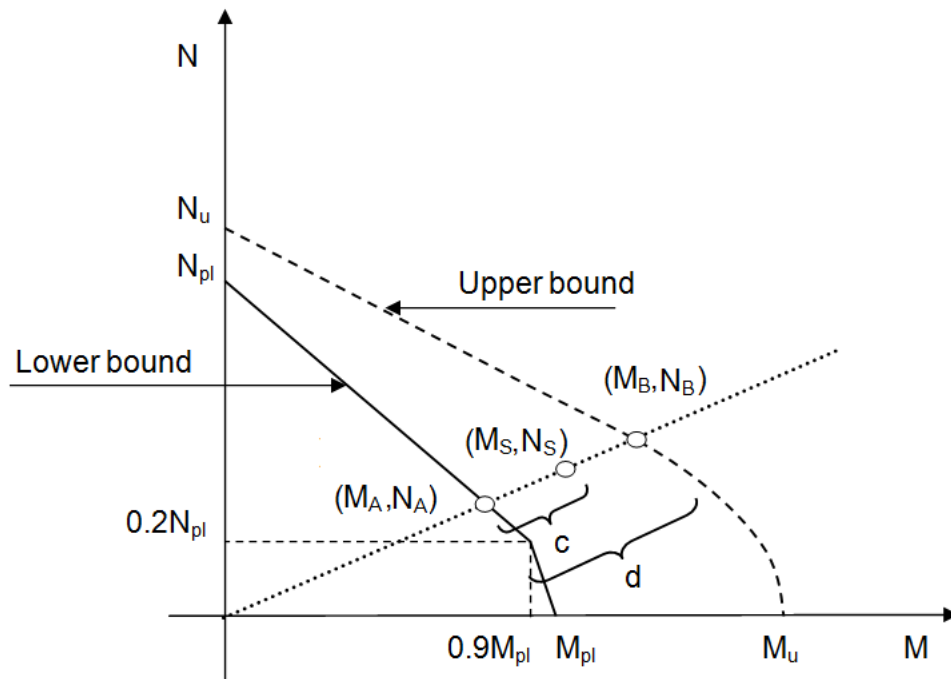
Figure 3

Figure 4

Figure 5

26

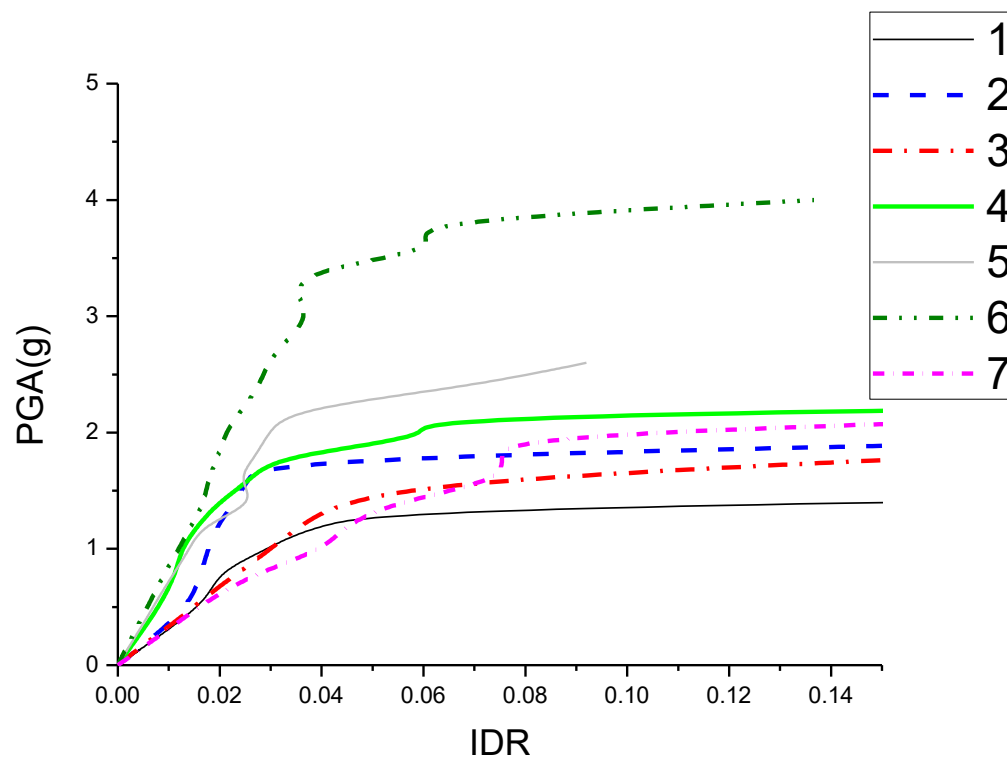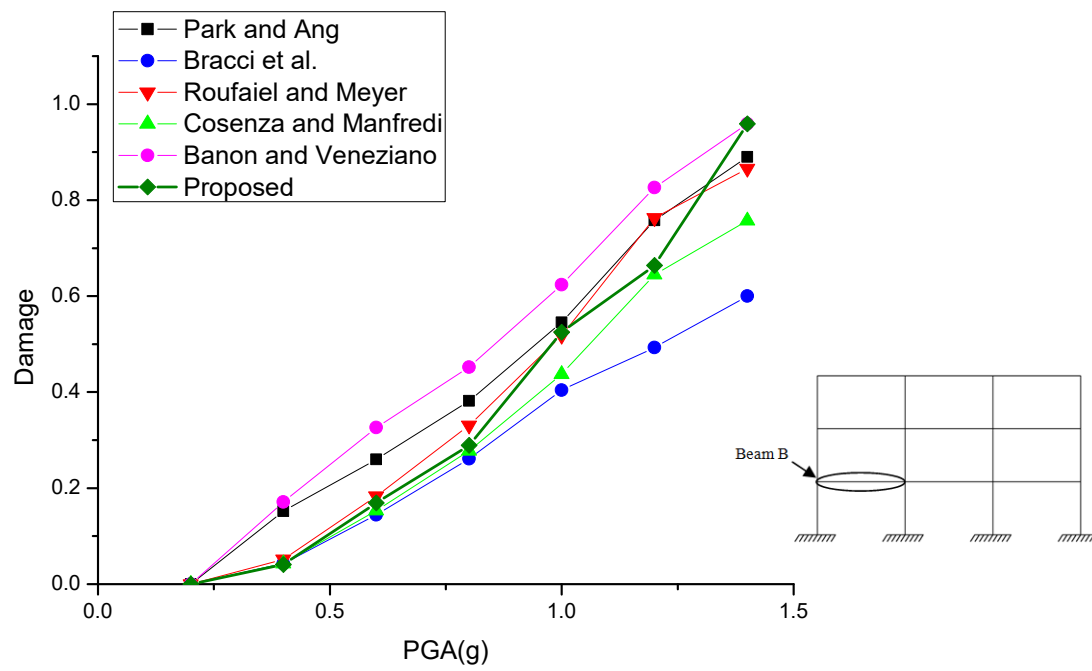Case 1
R=3.5, H=-3%, Whole sample
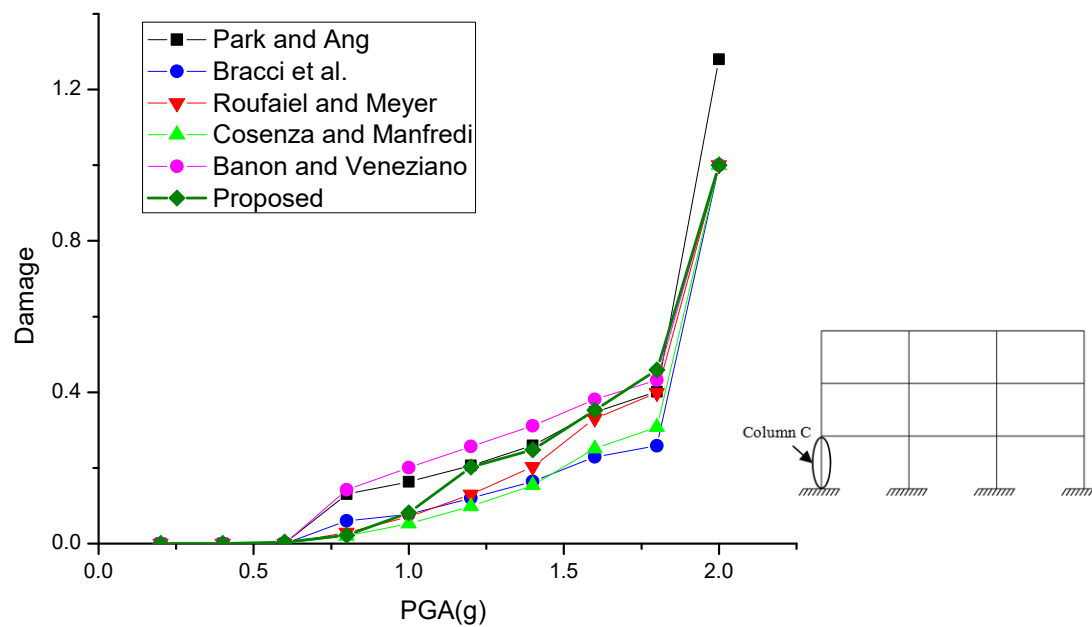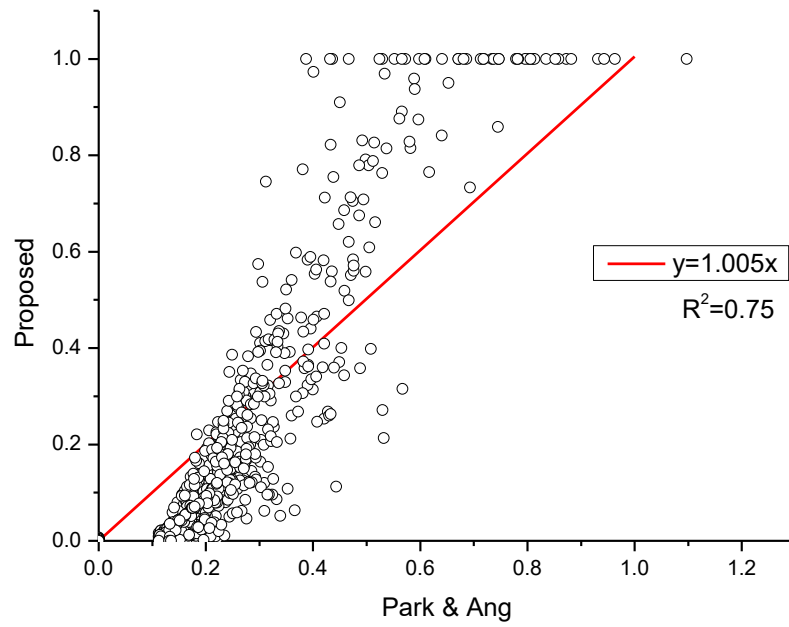ξ= 1.0% ξ= 2.0%
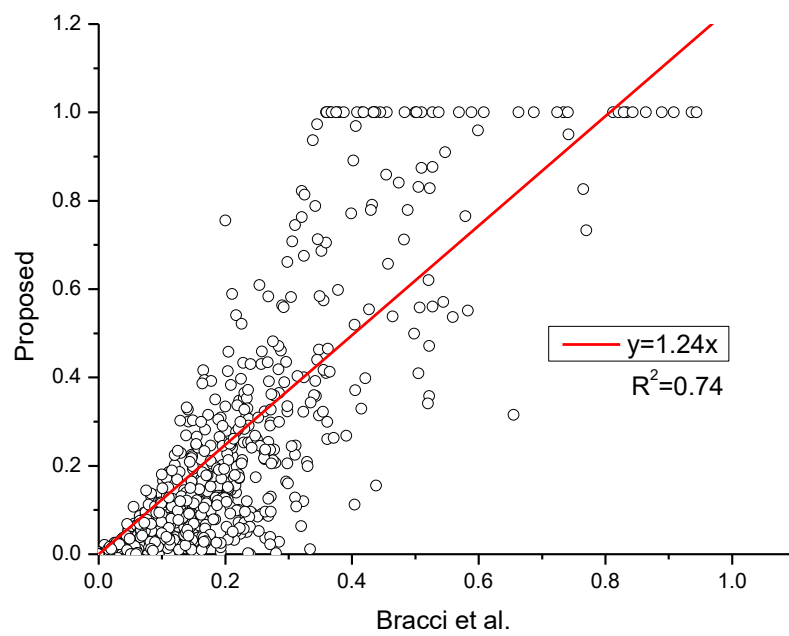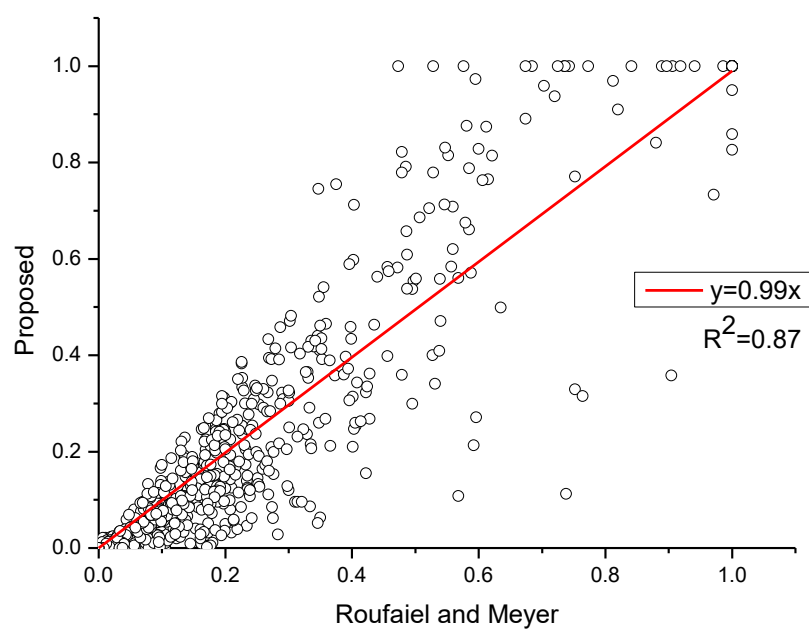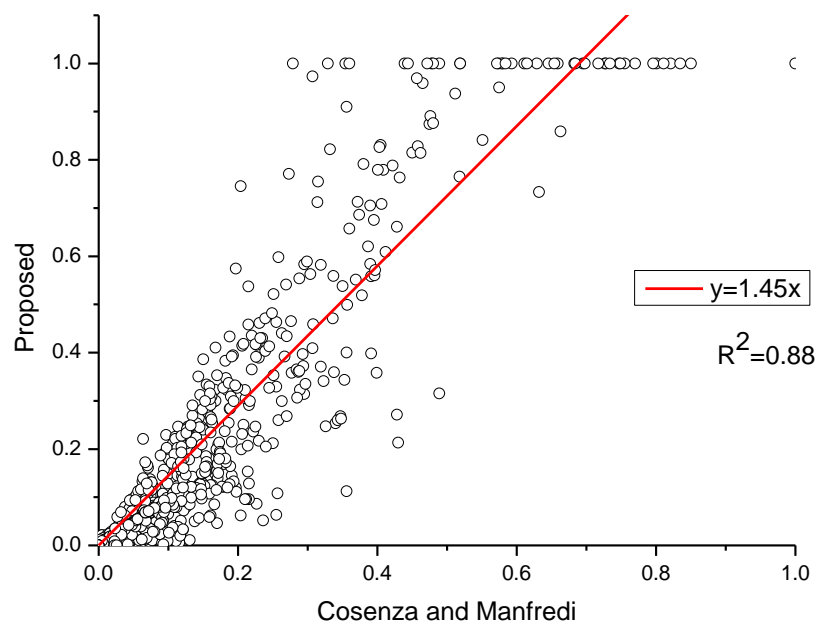ξ= 5.0% ξ=10.0%
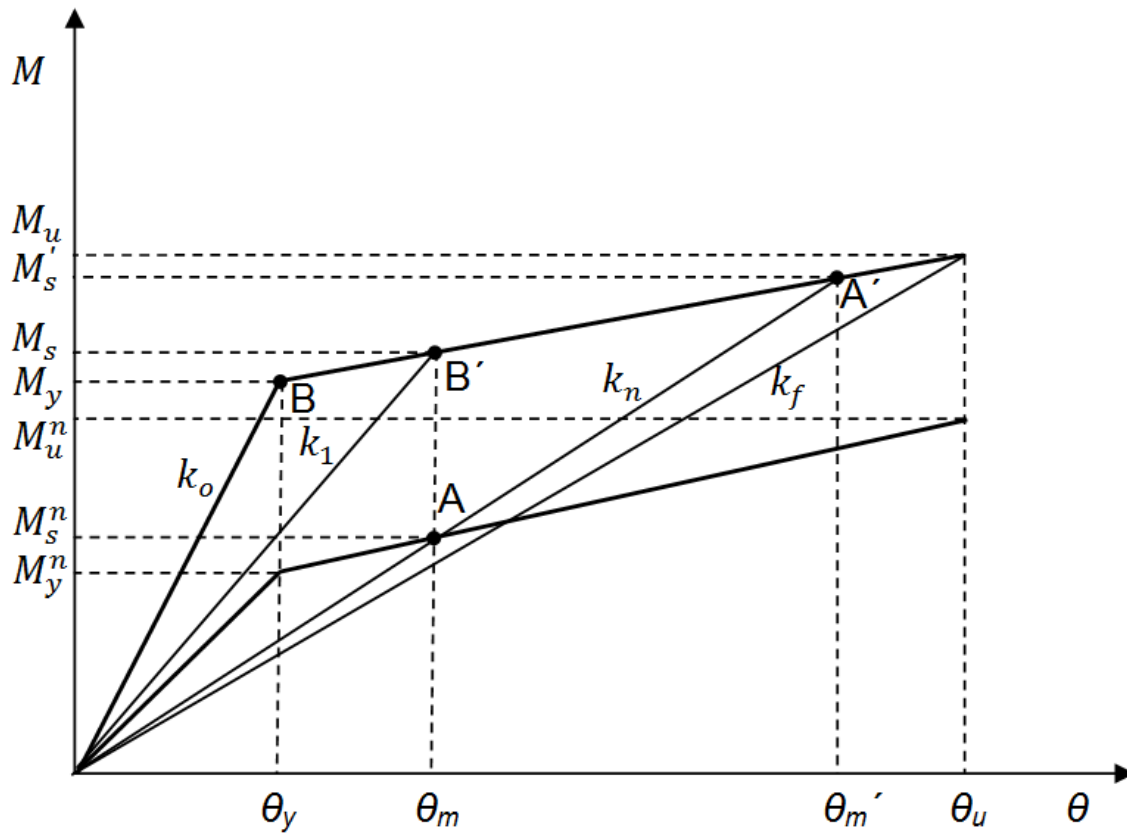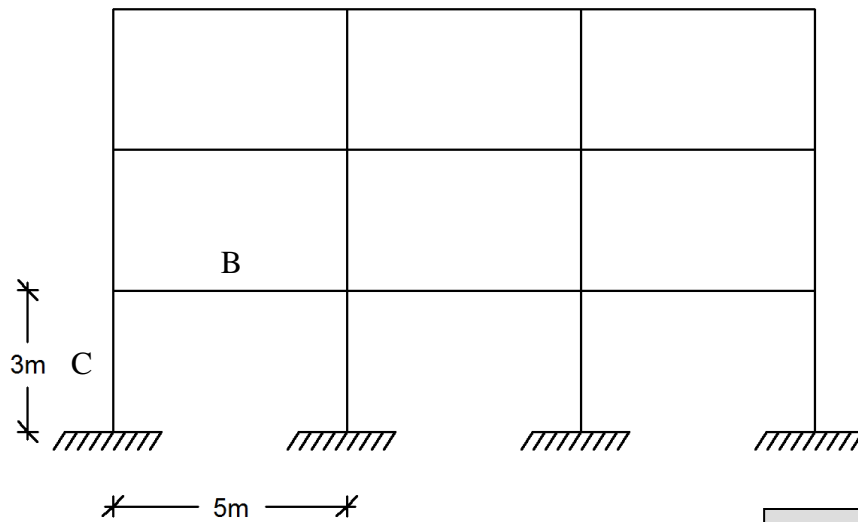
Figure 6
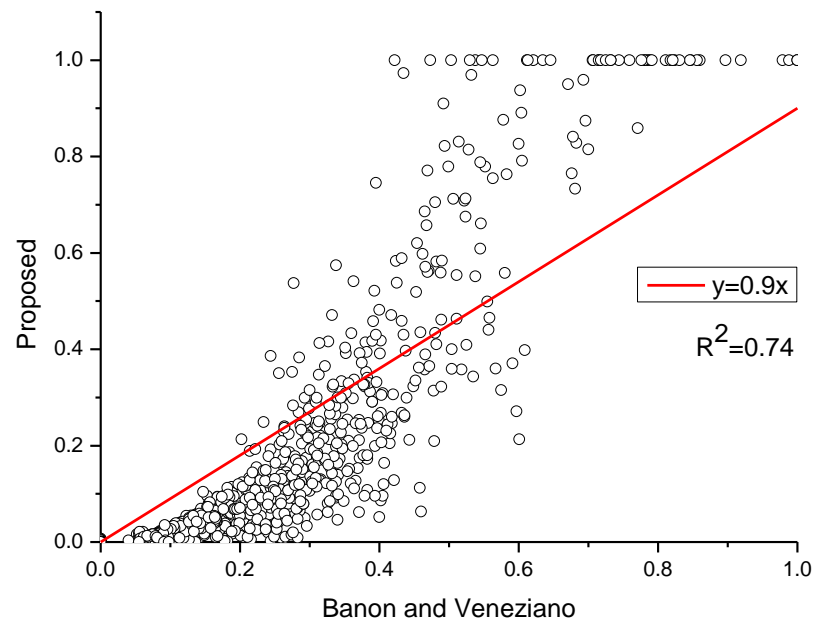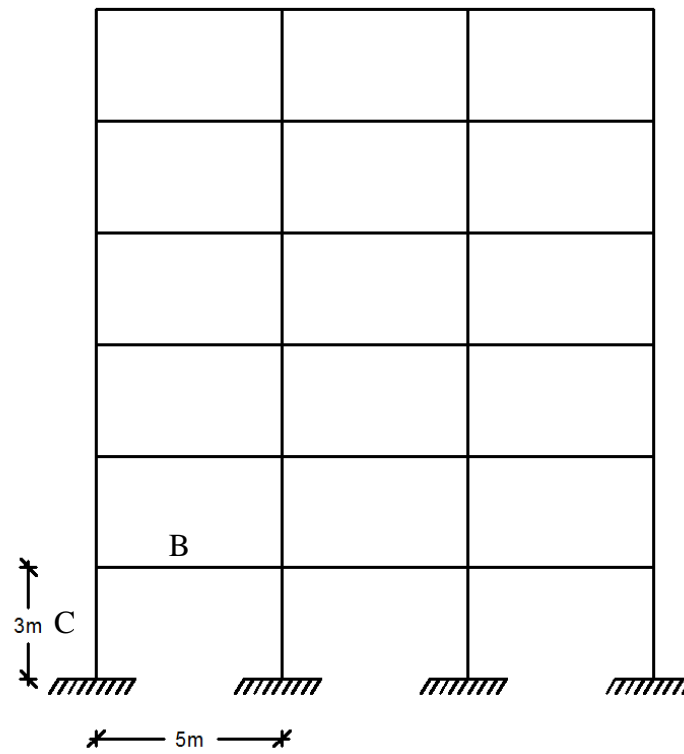
Figure 7

Figure 8

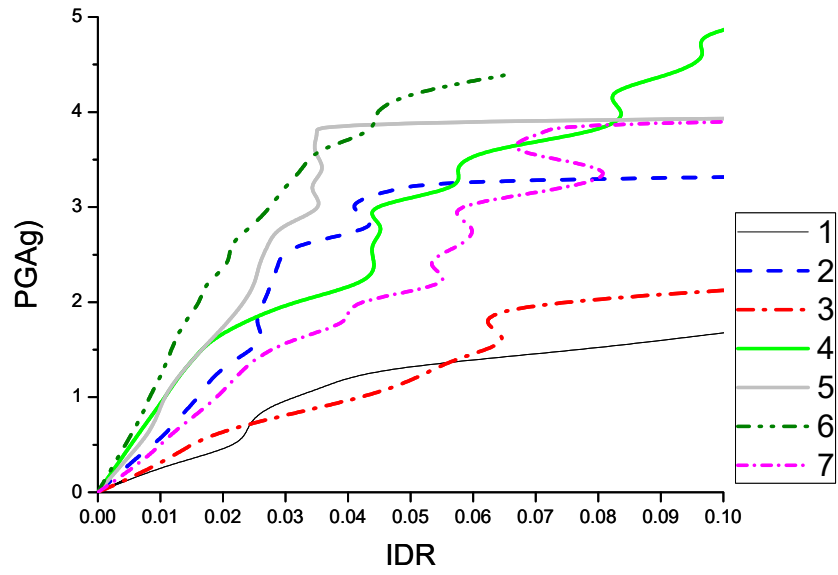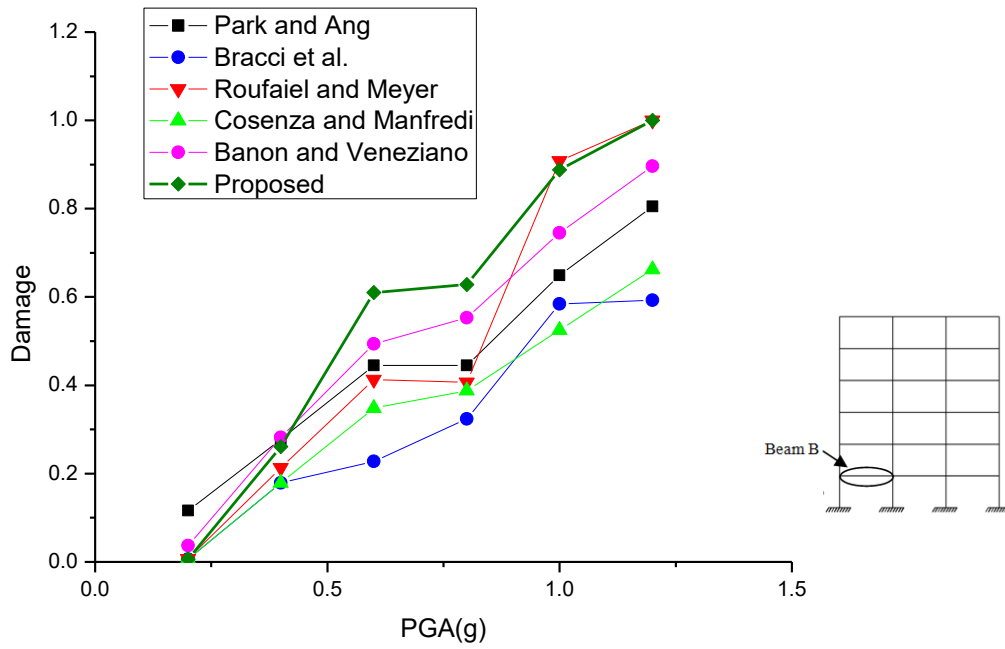Figure 9

Figure 10

Figure 11

Figure 12

Figure 13

Figure 14

Figure 15

Figure 16

Figure 17

Figure 18